

SCIENTIFIC REPORTS



OPEN

Local dynamics within the glass transition domain

François Godey, Alexandre Fleury & Armand Soldera 

The glass transition of an amorphous material is a fundamental property characterized by an abrupt change in viscosity. Its very knowledge was a conundrum as no satisfying theory existed at the molecular level. We herein relate this complex phenomenon to events occurring at the molecular scale. By studying conformational transitions in the carbon-chain polymer of polyethylene, we clearly establish a relation between local dynamics and the classical dihedral potential energy diagram of a carbon-carbon bond. This methodology is applied to a carbon-chain polymer with a side-group, polystyrene. A direct link is proved between activation energy and glass transition temperature. This work thus provides the cornerstone for linking molecular structure to macroscopic polymer properties, and in particular, the glass transition temperature.

Numerous systems such as polymers exhibit a glass transition. As the temperature is decreased they turn from an amorphous state of low viscosity to a supercooled liquid with very high viscosity¹. This transition is characterized by the glass transition temperature (T_g). Despite being known for a very long time it remains a thrilling domain of research as its very nature is not fully solved². The main reason is that no experiments or theories can grasp its entire domain of dynamic ranging from nanoseconds to years (ageing). These recent years, molecular simulation became an additional and powerful technique to complement existing data or current theories³. Among the different simulation tools, molecular dynamics simulation is of special interest as it can probe local dynamics. In 1988, Rigby and Roe, in their seminal work, showed that T_g can be extracted for polymers from full-atomistic simulation⁴. Since then, a huge number of simulations dealing with the glass transition of polymers have been reported^{5–7}. However, despite nice linear relationship between simulated and experimental T_g , as our group showed for instance⁸, the extremely rapid simulated cooling rate, in order of 10^{11} times more rapid than usual experiments, raise questions on its meaning. We thus propose, in this study, to shed some light on this issue by exploring the energy landscape, a powerful approach to deal with the glass transition. Consequently, a chemical picture of this tricky transition will emerge.

For decades, T_g was defined by the temperature at which the viscosity reaches 10^{13} poise^{1,9}. Nowadays, Differential Scanning Calorimetry (DSC) remains the most common technique to measure it by detecting change in the heat capacity of the sample occurring at the glass transition¹⁰. Dynamical Mechanical Analysis (DMA) is also greatly employed since it measures differences in viscoelasticity with temperature. Regardless the experimental technique, the temperature domain associated with the glass transition is in order of 3 to 5 K¹⁰. The most used simulation method to locate T_g is the dilatometry technique⁴. It consists in reporting the specific volume with respect to the temperature. The intersection between two linear fits at low and high temperatures gives T_g . However, we recently showed that due to the extremely rapid cooling rate, molecular dynamics (MD) simulation leads to a spreading of the glass transition domain, in order of 160 K¹¹. It was shown that the heat capacity and the coefficient of thermal expansion vary gradually between two limit temperatures, the lower (T_g^l) and the upper (T_g^u) transition temperatures. A comparison was then proposed with ultra-fast camera leading to the so-called overcranked effect where molecular features should be unveiled. Accordingly, behind the measurement of T_g from MD, the meaning of these two extra temperatures during the glass transition process must also be investigated. To unravel their significance, computing the activation energy (E_a) is a very attracting avenue as it depicts local dynamics^{12,13}. Moreover, it can be related to the energy landscape introduced by Angell¹⁴, and developed by Debenedetti and Stillinger¹⁵, one of the prevailing current theories to untangle the glass transition mystery.

In the energy landscape picture, a glass is trapped in a specific basin. The height of its barrier is directly related to the glass properties¹⁶. However, despite the very interesting outlook it brings, its depiction remains a challenging task. The activation energy corresponds to the energy necessary to go from one potential energy minimum to

Department of Chemistry, Centre Québécois sur les Matériaux Fonctionnels, Université de Sherbrooke, Sherbrooke, (Québec), J1K 2R1, Canada. Correspondence and requests for materials should be addressed to A.S. (email: Armand.Soldera@USherbrooke.ca)

Received: 23 November 2018

Accepted: 20 June 2019

Published online: 03 July 2019

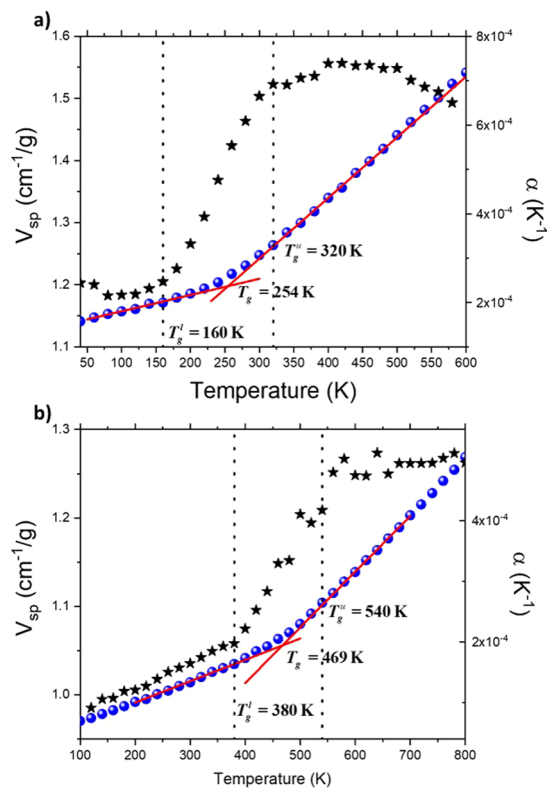


Figure 1. Specific volume (●) and thermal expansion coefficient (★) with respect to the temperature (K) for PE (a), and PS (b). The glass transition domain is limited by vertical dot lines at $160\text{ K } T_g^l$ and $320\text{ K } T_g^u$, and $380\text{ K } T_g^l$ and $540\text{ K } T_g^u$ for PE (a) and PS (b), respectively.

another inherent structure¹⁵. In polymers, it is numerically computed from an Arrhenius plot where frequencies of transitions between different rotameric states are reported with respect to the inverse of temperature^{13,17–19}. Nevertheless, the very interpretation of E_a stemming from MD simulation was source of interrogation²⁰. More specifically, an Arrhenius depiction of such relaxation remains surprising. It was suggested to be in relation with the computed potential energy barrier computed for the rotation of a single bond, in addition to be directly linked to T_g ²⁰. As pointed out by Boyd and Smith, “The resolution of these questions follows and leads to considerable insight into the nature of glass formation in polymer melts”²⁰. We thus propose to address the relationship between E_a and the temperatures associated with the glass transition, T_g , and the two temperature limits, through a description of a relevant portion of the potential energy landscape¹⁵. For this, two polymers are considered, one with the simplest architecture, polyethylene (PE), and one with a side-chain, polystyrene (PS). We then argue that an atomistic representation of the glass transition emerges.

Results and Discussion

To get numerical value of T_g , the simulated dilatometry technique is employed⁴. The specific volume is reported with respect to the temperature, as it is shown in Fig. 1a and b, for PE and PS, respectively. Values of T_g are 254 K and 469 K for PE and PS, respectively. The actual display of a discontinuity in the linear behavior of the specific volume with respect to the temperature is the sign of a change in the molecular behavior. However, as we recently reported, due to the very rapid cooling rate (in order of 10^{11} times more rapid than the experimental rate), this discontinuity is spread between two temperatures, a lower T_g^l and upper T_g^u , as revealed by the behavior of the thermal expansion coefficient (Fig. 1), the heat capacity⁴, or the bulk modulus²¹. It was argued that MD simulation acts as an ultra-fast camera leading to overcranking effects, enabling very slow-motion to be captured. This spread occurs between 160 K and 320 K, for PE (Fig. 1a), and 380 K and 540 K, for PS (Fig. 1b). For both polymers (Fig. 1), no changes in the behavior of the coefficient of thermal expansion are detected at T_g . The local dynamics is then investigated in the whole glass transition domain bounded by T_g^l and T_g^u . For this, the activation energy associated with the backbone motion is computed.

To establish the link between E_a extracted from an Arrhenius diagram, and the values of energies in the dihedral potential energy curve associated with the carbon-carbon bond, a reference is needed. We propose to use the following equation:

$$E_{\text{dihedral}}(\phi) = c_1[1 + \cos(\phi - \pi)] + c_2[1 - \cos(2(\phi - \pi))] + c_3[1 + \cos(3(\phi - \pi))]$$

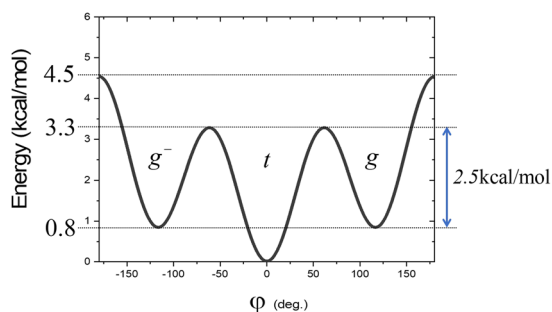


Figure 2. Dihedral potential energy for a carbon-carbon bond²¹.

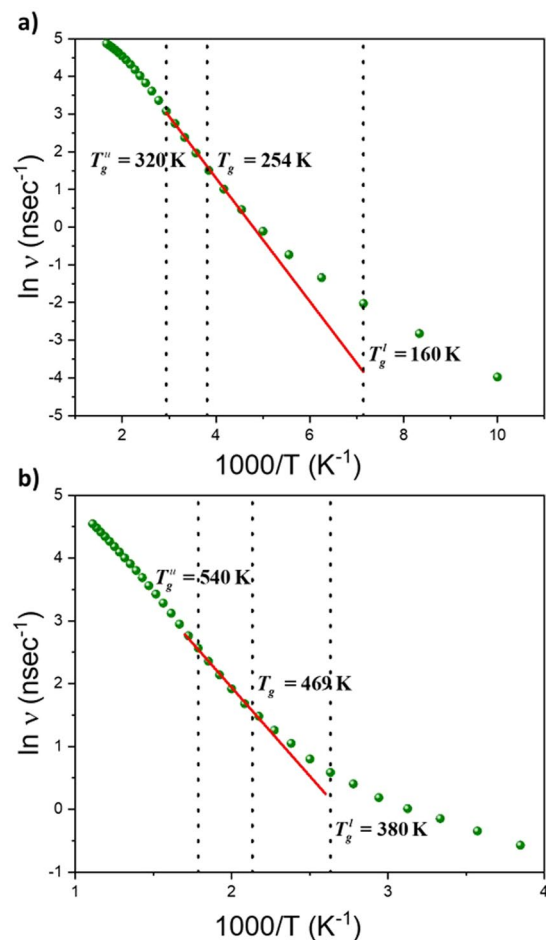


Figure 3. Arrhenius diagram for the all backbone transitions (●) for PE (a), and PS (b).

With the *trans* state is at 0 deg, and c_1 , c_2 , and c_3 , are coefficients whose values are 0.7055, -0.1355 , and 1.5722 kcal/mol respectively^{19,22}. The energetical diagram is displayed in Fig. 2. Three reference energies are indicated therein: energy of the *gauche* (*g* or *g*-) state, 0.8 kcal/mol, barrier heights to pass from the *trans* to *gauche* states, 3.3 kcal/mol, and to exchange the *gauche* states, 4.5 kcal/mol. The barrier height to go from a *gauche* state to the *trans* state is also indicated. Comparison with E_a stemming from the description of the polymer local dynamics can now be proceeded.

To compute E_a , the number of transitions between two rotameric states must first be established. It must be pointed out that all the reported data correspond to averages over eight configurations. The way a transition is registered was discussed in previous publications and summarized in the simulation methods paragraph¹³. Arrhenius diagrams for all transitions along the backbone chain in PE and PS are shown in Fig. 3.

E_a is directly extracted from the slope in the Arrhenius diagrams displayed in Fig. 3. The linear regression is made between T_g^i and T_g^u . A value of 3.2 kcal/mol for E_a for PE is supported by previous simulations and experimental data²³. Moreover, this value was usually suspected to be correlated with the actual potential energy barrier

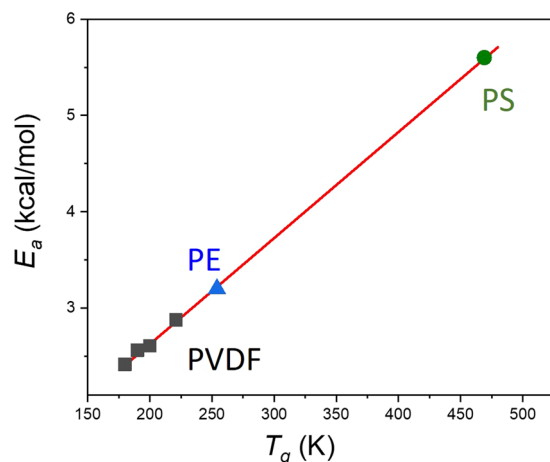


Figure 4. Activation energy (E_a in kcal/mol) with respect to the T_g of PVDFs (■)¹³, PE (▲) and PS (●).

necessary for a bond to go from the *trans* to *gauche* states, as shown in Fig. 2^{24–26}. It remains surprising that cooperative effects can be integrated in a value that corresponds to the simple barrier height between *trans* and *gauche* (Fig. 2). However, for PS, E_a is equal to 5.6 kcal/mol (Fig. 3b). This value should transcribe the cooperativity between side-chain and backbone motion as it is different from the potential energy height of a carbon-carbon bond (Fig. 2). It is in agreement with published data of 6 kcal/mol²⁷. Nevertheless, these values of E_a stemming from MD have been claimed by several authors including ourselves to be correlated with T_g ^{13,25}. These data have thus been inserted in the graph of $E_a(T_g)$ previously derived from polyvinylidene fluoride (PVDF) and its derivatives with different percentages of regioisomerism defects, in Fig. 4¹³. The additional data fit perfectly the linear regression arising from the previous data. The new linear regression is:

$$E_a(\text{kcal/mol}) = 0.01 \cdot T_g(\text{K}) + 0.44 \text{ kcal/mol}$$

with R^2 of 99.9%. The only difference with previous fitting equation lies in the ordinate at the origin, before 0.64 kcal/mol. Such a fit confirms the intimate relationships between T_g and E_a .

The linear relationship between E_a and T_g (Fig. 4) is of the utmost importance as it gives a molecular perspective of the nature of the glass structure. Accordingly, knowing E_a for each kind of backbone fragments of a polymer can lead to the computation of T_g stemming from simulated dilatometry, as we showed for E-PTFE¹³. Moreover, since E_a depicts local dynamics, it can be argued that T_g from MD is relevant to describe the backbone motion underlying the glass transition. 5.6 kcal/mol thus represents the activation energy associated with the backbone motion of the PS chain. However, in the case of PE, E_a is deduced from the simple barrier height between *trans* and *gauche* rotameric states (Fig. 2). This simple picture does not ultimately estimate cooperative effects²⁸. In fact, transitions reported in Fig. 3 include all kinds of transitions whatever the transition involves cooperative transition or local changes in the position of neighboring atoms. Separation between these two categories must be carried out.

Local dynamics is mainly governed by two types of motion: i) rotational transitions of backbone bonds from one rotameric state, i.e. *trans*, *gauche*, and *gauche*-, to another, and ii) librational motions about rotameric minima and fluctuations in bond lengths and bond angles²⁹. Intramolecular jumps in bond rotations associated with the backbone motion are actually due to librational motions^{29,30}. However, configurational transition referred as triggering transition³¹, can take place without resulting in large displacement of the whole polymer chain by two main mechanisms¹². (1) Cooperative transitions (CT) correspond to coupling of transition of closely-neighboring bonds along the chain. As a classical example, the crankshaft motion belongs to this category^{32,33}. (2) Isolated transitions (IT) do not lead to other dihedral transitions but distort surrounding atoms^{31,34}. Such transitions mainly occur at low temperatures³⁵. Their particularity is that they do not lead to a chain rearrangement, but a local alteration of atomic positions. Root means square displacements after an IT are shown in Figure of the Supporting Information, at 200 K, and agree published data³⁵. Percentages of these two transitions are then shown in Fig. 5 for both studied polymers.

T_g is set following an established protocol (Fig. 1). It does not correspond to a change in the coefficient of thermal expansion behavior. In Fig. 5, it can be observed that neither T_g nor T_g^u are indicative of any changes in the transition percentage. Conversely, T_g^l is the evidence of a change in the chain dynamics. Below this temperature, the number of both transitions remain roughly constant. While for PE, only isolated transitions occur in this domain, some cooperative transitions are detected for PS. The complexity of PS due to the presence of the side-chain should be accountable for their presence. Nevertheless, we can argue that T_g^l coincides with the beginning of cooperative motions as temperature is raised. Cooperative transitions below this transition temperature will not be considered in the rest of the text, in agreement with published data^{35,36}. As a result, the stemming activation energies should reflect the entire set of phenomena resulting in the occurrence of the glass transition process, giving insight into the chain dynamics, as outlined by de Gennes³⁷. Activation energy for the two kinds of transition can now be investigated.

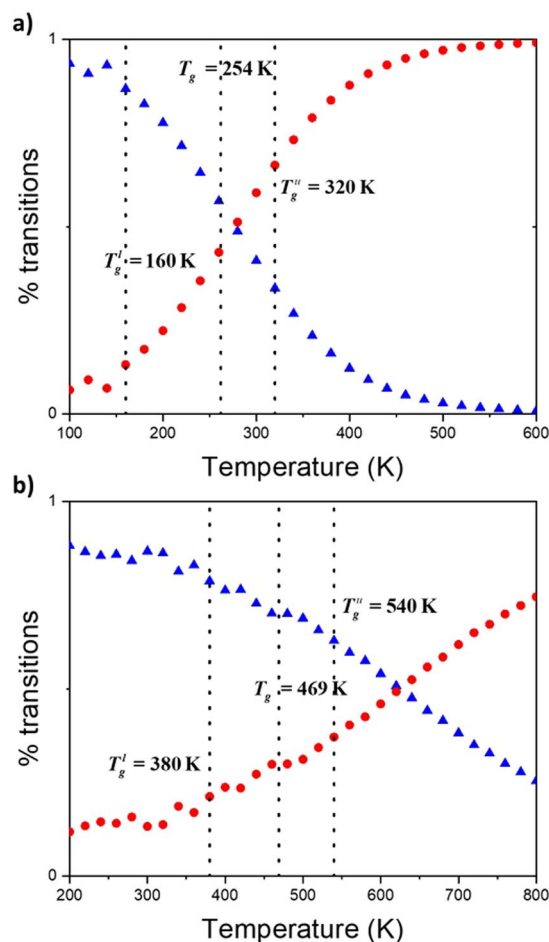


Figure 5. Percentage of cooperative (●) and isolated transitions (▲) with respect to temperature for PE (a) and PS (b). Vertical lines representing T_g , T_g^l and T_g^u are also shown.

Since there is clear variation in physical properties (coefficient of thermal expansion, specific volume and heat capacity) throughout the glass transition domain, between T_g^l and T_g^u , the activation energies were computed at each temperature to reveal any changes in the local dynamics. For this, the average of the two slopes associated with a frequency in the Arrhenius diagram is carried out. Three activation energies were thus considered: E_a^{at} stemming from the consideration of all backbone transitions (Fig. 3), E_a^{ct} coming from the cooperative transitions, and E_a^{it} extracted from isolated transitions which perturb only neighboring atomic positions. Their behavior with respect to temperature are displayed in Fig. 6 for both polymers.

General behavior of the different activation energies with respect to temperature (Fig. 6) are comparable for both polymers. The slight difference in the curve shape observed can origin from the presence of a bulky side-group in PS. Discussion on such effect request further development since cooperativity exists between the lateral group rotation and the backbone motion¹¹. Values of E_a^{at} associated with all the transitions are primarily investigated. The actual values stemming from the linear fit in the Arrhenius diagram (Fig. 3) correspond to the average of E_a^{at} in the graph of Fig. 6 between T_g and T_g^u . At this latter temperature, E_a^{ct} reaches a maximum value. A decrease after this temperature is observed. The reason for this behavior lies in the procedure to count transitions (cf *Simulation methods*). To be recognized as a transition, the new dihedral angle must not change during 1.5 ps. At high temperatures, especially at temperature higher than T_g^u , fluctuations increase leading to uncertainties in the definition of a transition. This simulation artifact is no further discussed as the focus is on describing the glass transition domain. At low temperatures, below T_g^l , behavior of E_a^{at} and E_a^{it} are merged. Only isolated transitions subsist, in agreement with previous conclusions from Fig. 5. This finding also agrees with published data: transitions can occur without any involvement of a rotation in neighboring bonds^{31,34}. An interesting statement is that for both polymers, values of E_a^{it} below T_g^l are equivalent, and equal to 1.5 kcal/mol. However, it is difficult to be certain about the unicity of this value since below T_g^l , the number of transitions is limited. Further studies on other polymers are needed. Nevertheless, we argue that it corresponds to the minimum potential energy required to generate one transition between rotameric states along a carbon backbone chain. Such an energy is not sufficient to prompt a transition in another bond (Fig. 2), and thus to engender cooperativity, but it is enough to involve changes in the position of neighboring atoms (Figure in the Additional Information).

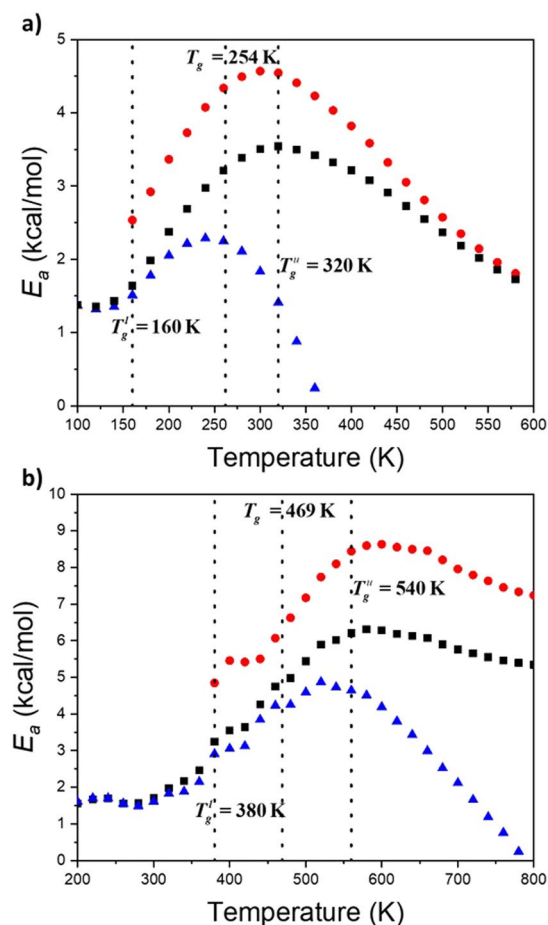


Figure 6. Activation energy (E_a) with respect to temperature stemming from the consideration of all backbone transitions, E_a^{at} (■), cooperative transitions, E_a^{ct} (●), and isolated transitions, E_a^{it} (▲), for PE (a), and PS (b).

The requested energy to generate a rotameric transition in another bond is E_a^{ct} at T_g^l where (i) curves of E_a^{at} and E_a^{it} split (Fig. 6) and (ii) percentage of CT begins to increase (Fig. 5). At T_g^l , the value of E_a^{ct} is 2.5 kcal/mol and in order of 5 kcal/mol for PE and PS, respectively. For PE, this latter value corresponds exactly to the barrier height between *gauche* and *trans* states (Fig. 2). Based on previous correlation (Fig. 4), we can thus claim that 5 kcal/mol is the potential energy height for *gauche* to *trans* transition in PS along the backbone chain with a phenyl side-group. At T_g^u , E_a^{ct} reaches its maximum value. These values are 4.5 kcal/mol and 8.6 kcal/mol for PE and PS, respectively. For PE, this value corresponds to the total energy barrier height (Fig. 2). From all the information gained from the study of the activation energies, a simple atomistic picture of the glass transition can be retrieved. It is displayed in Fig. 7. The values of the energy are associated with those stemming from PE but can be transferred to PS and other polymers.

In summary, the chemical pictures of the two limit temperatures, and the resulting domains of temperatures (Fig. 7) are as follows:

- $T < T_g^l$: Transitions between rotameric states mainly lead to changes in neighboring atoms position.
- T_g^l : Temperature at which there is enough potential energy for transitions between rotameric states to generate rotation in another dihedral angle. This energy corresponds to the barrier height to go from *gauche* to *trans* states.
- $T_g^l < T < T_g^u$: Domain of cooperativity between two bonds, i.e. changes in rotameric states are achieved between two bonds along the polymer chain.
- T_g^u : Temperature corresponding to the maximum of the potential energy barrier.
- $T_g^u < T$: Domain of more complex cooperativity.

Conclusion

Due to very rapid cooling rate, molecular dynamics simulation leads to a spread in the glass transition domain bordered by a lower (T_g^l) and an upper (T_g^u) temperatures. The actual enlargement has been seen as an overcranking effect as the coefficient of thermal expansion and the heat capacity vary progressively¹¹. However, it challenges the very definition of T_g from atomistic simulation, as it corresponds to an intersection between two linear fits in the dilatometry simulation,

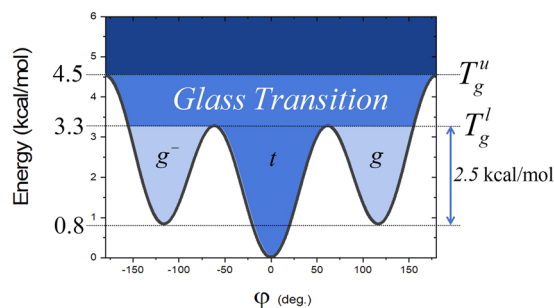


Figure 7. Torsional potential energy with respect to the dihedral angle associated with a C-C bond along the backbone chain with correspondance between energy values and T_g^l and T_g^u .

not to a change in physical properties. To address this important issue, local dynamics of two polymers, polyethylene (PE) and polystyrene (PS), was investigated thanks to the computation of the activation energy, E_a .

By confronting computed activation energies with previously published values of E_a stemming from PVDF derivatives, we clearly demonstrated that E_a is directly related to T_g . This value corresponds to a single barrier height in dihedral potential energy diagram. To better grasp the meaning of E_a extracted from the consideration of the backbone transitions, two different kind of transitions were considered: isolated and cooperative transitions. For the former ones, it was shown that they are mainly exhibited at low temperatures in agreement with published studies. It is worth noting that both polymers exhibit the same E_a , 1.5 kcal/mol. We argue that this value corresponds to the minimum potential energy required to generate one transition between rotameric states along a carbon backbone chain. However, the unique value for PE and PS cannot be generalized at this point. Further studies are needed. At T_g^l , alternative transitions at another bond come into play. The associated E_a is 2.5 kcal/mol which corresponds to the potential energy for a *gauche* state to go in a *trans* state, in the dihedral potential energy diagram. The maximum value is reached at T_g^u where E_a is 4.5 kcal/mol for PE which is the maximum energy in the dihedral potential energy carbon-carbon. For PS, these values are 5 and 8.6 kcal/mol respectively. We thus clearly answer the question raised by Boyd in effect that does E_a behavior appropriate to a single barrier height or whether higher values might arise due to cooperative effect. Accordingly, a simple atomistic picture of the glass transition was shown. This atomic representation should be applied to other systems for which particular behaviour at the glass transition has been reported such as thin films³⁸.

Methods

More details of the whole molecular simulation procedure to get T_g can be found in previous articles^{39–41}. Selection of the initial configurations and their relaxation process are crucial. A cell with periodic boundary conditions is constituted by a chain of 250 monomers long for PE, and 125 monomers long for PS. The generation of the chains imbedded in the cell was done through the Self-Avoiding Walk procedure of Theodorou-Suter⁴² and Meirovitch⁴³ scanning methods, implemented in the Amorphous_Cell© code, in the Materials Studio environment. 50 configurations were thus first obtained. A first selection was made by considering their radius of gyration not to stray too far from the average value. Second, 8 configurations with the lowest energy are finally selected. A heating-cooling process was then employed to eliminate any endemic stress. Molecular dynamics (MD) in the NPT (i.e., constant number of particles, pressure, and temperature) ensemble was used. The integration of Newton's equation of motion was performed using the velocity Verlet integration algorithm with a 1 fs integration time step⁴⁴. The Nosé-Hoover thermostat and Parrinello-Rafman barostat algorithms were used to maintain constant temperatures and pressures, respectively^{45,46}. The *pcff* force field was chosen. The non-bonded interactions have been computed using the Ewald summation, to take into account long-range effects³. All the MD simulations have been carried out using the LAMMPS code⁴⁷. The heating-cooling process consists in a fast heating process (50 K/200 ps) followed by a lower cooling rate (20 K/ns). It has been shown that to get reproducible values of T_g , the initial configuration must be in mechanical equilibrium, a “quasi-static” equilibrium state where the stress in the cell balances the internal pressure⁴⁸. A uniform hydrostatic compression is imposed to the system until the internal energy reaches a minimum. During the cooling down process, 20 K/ns, the specific volume is reported with respect to the temperature, for each ensuing configuration. This simulated dilatometry leads to the value of T_g . MD of 10 ns are then run at each temperature, and a configuration is saved at each 500 fs.

Details concerning the calculation of E_a can be found in a previous publication. The important initial step is to account for a transition. The method we used can be summarized into 4 key points. The procedure corresponds to a slightly modified Wu's procedure¹⁸. (1) Fluctuations in the dihedral angle around the rotameric states are smoothed by a sliding average. (2) In order for a transition to be identified, the difference between the two involved dihedral angles must be greater than 40 deg. (3) The time interval that is requested for a new state along a trajectory to lose memory of its previous state was set at 3 ps. (4) The torsion angle of the new rotameric state must exist for more than 1.5 ps to avoid counting abrupt changes of states.

References

1. Donth, E.-J. *The Glass Transition*. **48**, (Springer Berlin Heidelberg, 2001).
2. Ngai, K. L. Why the glass transition problem remains unsolved? *J. Non. Cryst. Solids* **353**, 709–718 (2007).
3. Allen, P. & Tildesley, D. J. *Computer simulation of liquids-2nd Edition*. (Oxford University Press, 2017).

4. Rigby, D. & Roe, R.-J. Molecular dynamics simulation of polymer liquid and glass. II. Short range order and orientation correlation. *J Chem Phys* **89**, 5280 (1988).
5. Binder, K., Baschnagel, J. & Paul, W. Glass transition of polymer melts: test of theoretical concepts by computer simulation. *Prog. Polym. Sci.* **28**, 115–172 (2003).
6. Wu, C. Re-examining the procedure for simulating polymer T_g using molecular dynamics. *J. Mol. Model.* **23**, 270 (2017).
7. Gee, R. H. & Boyd, R. H. The role of the torsional potential in relaxation dynamics: a molecular dynamics study of polyethylene. *Comput. Theor. Polym. Sci.* **8**, 93–98 (1998).
8. Soldera, A. & Metatla, N. Glass transition of polymers: Atomistic simulation versus experiments. *Phys. Rev. E* **74**, 61803 (2006).
9. Sperling, L. H. *Introduction to Physical Polymer*. (John Wiley & Sons, Inc., 2006).
10. Wunderlich, B. *Thermal Analysis of Polymeric Materials*. (Springer, 2005).
11. Godey, F., Fleury, A., Ghoufi, A. & Soldera, A. The extent of the glass transition from molecular simulation revealing an overcrank effect. *J. Comput. Chem.* <https://doi.org/10.1002/jcc.25069> (2017).
12. Takeuchi, H. & Roe, R.-J. Molecular dynamics simulation of local chain motion in bulk amorphous polymers. II. Dynamics at glass transition. *J. Chem. Phys.* **94**, 7458 (1991).
13. Anousheh, N., Godey, F. & Soldera, A. Unveiling the impact of regioisomerism defects in the glass transition temperature of PVDF by the mean of the activation energy. *J. Polym. Sci. Part A Polym. Chem.* **55**, 419–426 (2017).
14. Angell, A. Liquid landscape. *Nature* **393**, 521 (1998).
15. Debenedetti, P. G. & Stillinger, F. H. Supercooled liquids and the glass transition. *Nature* **410**, 259–67 (2001).
16. Parisi, G. & Sciortino, F. Structural glasses: Flying to the bottom. *Nat. Mater.* **12**, 94–5 (2013).
17. Hotston, S. D., Adolf, D. B. & Karatasos, K. An investigation into the local segmental dynamics of polyethylene: An isothermal/isobaric molecular dynamics study. *J. Chem. Phys.* **115**, 2359 (2001).
18. Wu, R., Zhang, X., Ji, Q., Kong, B. & Yang, X. Conformational transition behavior of amorphous polyethylene across the glass transition temperature. *J. Phys. Chem. B* **113**, 9077–9083 (2009).
19. Liang, T., Yang, Y., Guo, D. & Yang, X. Conformational transition behavior around glass transition temperature. *J. Chem. Phys.* **112**, 2016–2020 (2000).
20. Boyd, R. H. & Smith, G. D. *Polymer Dynamics and Relaxation*. (Cambridge University Press, 2007).
21. Godey, F., Bensaid, M. O. & Soldera, A. Extent of the glass transition in polymers envisioned by computation of mechanical properties. *Polymer* **164**, 33–38 (2019).
22. Harmandaris, V. A., Adhikari, N. P., Van Der Vegt, N. F. A. & Kremer, K. Hierarchical modeling of polystyrene: From atomistic to coarse-grained simulations. *Macromolecules* **39**, 6708–6719 (2006).
23. Kanaya, T., Kaji, K. & Inoue, K. Local Motions of Cis-1,4-Polybutadiene in the Melt - a Quasi-Elastic Neutron-Scattering Study. *Macromolecules* **24**, 1826–1832 (1991).
24. Adolf, D. B. & Ediger, M. D. Brownian dynamics simulations of local polymer dynamics. *Macromolecules* **24**, 5834–5842 (1991).
25. Wu, R., Kong, B. & Yang, X. Conformational transition characterization of glass transition behavior of polymers. *Polymer* **50**, 3396–3402 (2009).
26. Boyd, R. H., Gee, R. H., Han, J. & Jin, Y. Conformational dynamics in bulk polyethylene: A molecular dynamics simulation study. *J. Chem. Phys.* **101**, 788 (1994).
27. Lačević, N. *et al.* Spatially heterogeneous dynamics investigated via a time-dependent four-point density correlation function. *J. Chem. Phys.* **119**, 7372–7387 (2003).
28. Pant, P. V. K., Han, J., Smith, G. D. & Boyd, R. H. A molecular dynamics simulation of polyethylene. *J. Chem. Phys.* **99**, 597 (1993).
29. Baysal, C., Atilgan, A. R., Erman, B. & Bahar, İ. Molecular Dynamics Analysis of Coupling between Librational Motions and Isomeric Jumps in Chain Molecules. *Macromolecules* **29**, 2510–2514 (1996).
30. Moro, G. J. The coupling between librational motions and conformational transitions in chain molecules. II. The rotor chain represented by the master equation for site distributions. *J. Chem. Phys.* **97**, 5749 (1992).
31. Moe, N. E. & Ediger, M. D. Computer simulations of polyisoprene local dynamics in vacuum, solution, and the melt: Are conformational transitions always important? *Macromolecules* **29**, 5484–5492 (1996).
32. Helfand, E., Wasserman, Z. R. & Weber, T. A. Brownian dynamics study of polymer conformational transitions. *J. Chem. Phys.* **70**, 2016–2017 (1979).
33. Helfand, E., Wasserman, Z. & Weber, T. Brownian Dynamics Study of Polymer Conformational Transitions. *Macromolecules* **13**, 526–533 (1980).
34. Starkweather, H. W. Noncooperative Relaxations. *Macromolecules* **21**, 1798–1802 (1988).
35. Bahar, I., Erman, B. & Monnerie, L. Kinematics of Polymer Chains with Freely Rotating Bonds in a Restrictive Environment. 1. Theory. *Macromolecules* **25**, 6309–6314 (1992).
36. Haliloglu, T., Bahar, I., Erman, B. & Mattice, W. L. Relative Contributions of Coupled Rotations and Small-Amplitude Torsions to Conformational Relaxation in Polymers. **9297**, 8942–8947 (1996).
37. de Gennes, P. G. *Scaling concepts in polymer physics*. (Cornell University Press, 1979).
38. El Ouakili, A., Vignaud, G., Balnois, E., Bardeau, J. F. & Grohens, Y. Multiple glass transition temperatures of polymer thin films as probed by multi-wavelength ellipsometry. *Eur. Phys. J. Appl. Phys.* **519**, 2031–2036 (2011).
39. Soldera, A. Atomistic simulations of vinyl polymers. *Mol. Simul.* **38**, 762–771 (2012).
40. Metatla, N. & Soldera, A. Computation of densities, bulk moduli and glass transition temperatures of vinylic polymers from atomistic simulation. *Mol. Simul.* **32**, 1187–1193 (2006).
41. Metatla, N. & Soldera, A. The Vogel-Fulcher-Tammann equation investigated by atomistic simulation with regard to the Adam-Gibbs model. *Macromolecules* **40**, 9680–9685 (2007).
42. Theodorou, D. N. & Suter, U. W. Detailed molecular structure of a vinyl Polymer glass. *Macromolecules* **18**, 1467–1478 (1985).
43. Meirovitch, H. Computer simulation of self-avoiding walks: Testing the scanning method. *J Chem Phys* **79**, 502 (1983).
44. Haile, J. M. *Molecular Dynamics Simulation*. (John Wiley & Sons, 1992).
45. Victor, R. Berendsen and Nose-Hoover thermostats Temperature in MD MD at constant Temperature - NVT ensemble 1–4 (2007).
46. Parrinello, M. & Rahman, A. Strain fluctuations and elastic constants. *J. Chem. Phys.* **76**, 2662 (1982).
47. Plimpton, S. Fast parallel algorithms for short-range molecular dynamics. *J. Comput. Phys.* **117**, 1–19 (1995).
48. Metatla, N. & Soldera, A. Effect of the molar volume on the elastic properties of vinylic polymers: A static molecular modeling approach. *Macromol. Theory Simulations* **20**, 266–274 (2011).

Acknowledgements

The computational resources were provided by Calcul Québec and Compute Canada, through the financial support of the Canadian Foundation Innovation (CFI). This work was supported by the Université de Sherbrooke, the Fonds Québécois de la Recherche sur la Nature et les Technologies (FRQNT), and the Natural Sciences and Engineering Research Council of Canada (NSERC).

Author Contributions

A.S. designed the research and wrote the manuscript. F.G. performed the simulations. A.F. computed the MSD. All the authors revised and proof read the paper.

Additional Information

Supplementary information accompanies this paper at <https://doi.org/10.1038/s41598-019-45933-2>.

Competing Interests: The authors declare no competing interests.

Publisher's note: Springer Nature remains neutral with regard to jurisdictional claims in published maps and institutional affiliations.



Open Access This article is licensed under a Creative Commons Attribution 4.0 International License, which permits use, sharing, adaptation, distribution and reproduction in any medium or format, as long as you give appropriate credit to the original author(s) and the source, provide a link to the Creative Commons license, and indicate if changes were made. The images or other third party material in this article are included in the article's Creative Commons license, unless indicated otherwise in a credit line to the material. If material is not included in the article's Creative Commons license and your intended use is not permitted by statutory regulation or exceeds the permitted use, you will need to obtain permission directly from the copyright holder. To view a copy of this license, visit <http://creativecommons.org/licenses/by/4.0/>.

© The Author(s) 2019